# Erosions and Fatty Lesions of Sacroiliac Joints in Patients with Axial Spondyloarthritis: Evaluation of Different MRI Techniques and Two Scoring Methods

Michaela Krohn, Leonie S. Braum, Joachim Sieper, In-Ho Song, Anja Weiß, Johanna Callhoff, Christian E. Althoff, Bernd Hamm, and Kay-Geert A. Hermann

*ABSTRACT.* ***Objective.*** Assessment of structural damage of sacroiliac joints (SIJ) in patients with axial spondyloarthritides (axSpA) has been discussed as a useful outcome measure in clinical trials. The aim of our study was to evaluate different magnetic resonance imaging (MRI) scoring methods and pulse sequences with a focus on fatty lesions and bony erosions.

***Methods.*** Seventy-five patients with the diagnosis of axSpA underwent MRI at 3 timepoints as part of the ESTHER trial, which compared 2 groups of patients treated with etanercept or sulfasalazine. Two MRI sequences [unenhanced T1-weighted (T1w) turbo spin-echo (TSE) and unenhanced T1w opposed-phase gradient-echo sequences (opGRE)] and 2 different scoring systems (simple and comprehensive Berlin method) were used for the evaluation of fatty lesions and erosions of the SIJ. Differences between techniques and methods were evaluated by intraclass correlation coefficients (ICC) and standardized response means (SRM).

***Results.*** Applying the simple Berlin method, mean fatty lesion scores for etanercept-treated patients were 4.59 and 5.19 at baseline and Week 48, respectively, while the comprehensive Berlin method revealed mean fatty lesion scores of 6.59 and 7.64, respectively. Corresponding SRM were 0.59 and 0.86 for simple and comprehensive methods, respectively, while ICC dropped from 0.76–0.77 to 0.59–0.62. Scoring of erosions on T1w opGRE images resulted in a higher interreader agreement (ICC of 0.65) compared to T1w TSE sequences (ICC of 0.18).

***Conclusion.*** Better characterization of fatty lesion changes within 1 year was achieved by the comprehensive Berlin scoring method; however, more reader variation has to be taken into account. The delineation of erosions is markedly improved when using T1w opGRE pulse sequences. (J Rheumatol First Release Feb 1 2014; doi:10.3899/jrheum.130581)

*Key Indexing Terms:*
SACROILIAC JOINTS MAGNETIC RESONANCE IMAGING SACROILIITIS
AXIAL SPONDYLOARTHRITIS ANKYLOSING SPONDYLITIS SCORING SYSTEM

Axial spondyloarthritides (axSpA) are a group of various rheumatic diseases with an overall prevalence of 1.9%, of which ankylosing spondylitis is the most important[1,2,3]. Recently, classification criteria of axSpA have been revised by the Assessment of SpondyloArthritis international Society (ASAS)[4]. These criteria incorporate (besides HLA-B27 testing) imaging of the sacroiliac joints (SIJ) as 1 of the key features of axSpA. While active inflammation is detected by magnetic resonance imaging (MRI), conventional radiographs are still used to characterize structural damage such as erosions, sclerosis, or ankylosis[4,5]. However, the progression of these structural osseous changes is very slow, indicating that conventional radiographs are useful neither to confirm the diagnosis of early axSpA nor as an outcome measure in clinical trials. Structural damage lesions of the SIJ on MRI have previously been defined by ASAS experts[6], but there seems to be uncertainty about the reliability of their detection on MRI[7,8,9,10]. Erosions of the SIJ have been shown to be of high value for the diagnosis of axSpA[11]. The combined detection of erosions and periarticular osteitis seems to increase the sensitivity of MRI to some extent[12,13].

Another focus of particular scientific interest in axSpA is the transition of inflammatory lesions into fatty lesions. Fatty lesions are not detectable on conventional radiographs or computed tomography, whereas MRI may even detect small areas of fat deposition[14,15]. However, it remains unclear which role fatty lesions play in the context of disease chronicity because it has been considered part of the

*From the Charité Medical School, Department of Radiology, and Medical Department of Infectiology, Gastroenterology, and Rheumatology; and the German Rheumatology Research Centre, Berlin, Germany.*

*M. Krohn, MD; L.S. Braum, MD, Charité Medical School, Department of Radiology; J. Sieper, MD, PhD; I-H. Song, MD, PhD, Charité Medical School, Medical Department of Infectiology; A. Weiß, MSc; J. Callhoff, MSc, German Rheumatology Research Centre; C.E. Althoff, MD; B. Hamm, MD, PhD; K-G.A. Hermann, MD, PhD, Charité Medical School, Department of Radiology.*

*Address correspondence to Dr. K.G. Hermann, Charité Medical School, Department of Radiology, Charitéplatz 1, 10117 Berlin, Germany. E-mail: kgh@charite.de*

*Accepted for publication November 29, 2013.*

Personal non-commercial use only. The Journal of Rheumatology Copyright © 2014. All rights reserved.



Downloaded on April 16, 2024 from www.jrheum.org

reparative processes[16,17], while a current study suggests a positive correlation of fatty lesions and subsequent new bone formation[18].

Altogether, reliable MRI sequences and suitable scoring systems for the detection and quantification of erosions and fatty lesions are warranted to reliably evaluate structural osseous changes in the course of disease or when evaluating new pharmaceutical agents; initial investigations are promising[19]. The aim of our study was to weigh 2 different MRI scoring methods and pulse sequences with a focus on fatty lesions and bony erosions.

## MATERIALS AND METHODS

*Patients*. Our study is part of a prospective, randomized multicenter trial that was approved by an independent ethics committee. All patients included had active axSpA with a symptom duration of ≤ 5 years and were randomly assigned to an etanercept or sulfasalazine (SSZ) treatment group[20]. The diagnosis of axSpA was made based on the presence of chronic low back pain for ≥ 3 months and symptom onset at < 45 years of age. All patients had to show active inflammation (osteitis/bone marrow edema) on whole-body MRI, either on SIJ or the spine, plus 3 established clinical criteria according to the ASAS classification[4,6,20]. A detailed description of inclusion and exclusion criteria has been published[20].

All patients had a whole-body MRI examination at 3 timepoints (A: baseline; B: Week 24; C: Week 48). Altogether, 65 patients (etanercept group: n = 35; SSZ group: n = 30) completed the study; dropouts have been described[16,20].

*MRI examination*. All patients underwent a whole-body MRI examination on a 1.5 Tesla MR scanner (Avanto TIM) according to an established examination protocol[20,21,22]. The examination was performed in a supine position using a whole-body surface coil system. For our study, unenhanced T1-weighted (T1w) turbo spin-echo (TSE) and opposed-phase gradient-echo (opGRE) sequences of the SIJ were analyzed. Both sequences were acquired in oblique coronal orientation along the long axis of the sacral bone with a matrix size of 512 × 512 pixels and a slice thickness of 3 mm. T1w TSE sequences were acquired with a field of view (FOV) of 310 mm, a repetition time (TR) of 790 ms, an echo time (TE) of 19 ms, and a flip angle of 150°; opGRE sequences were performed with an FOV of 260 mm, a TR of 180 ms, a TE of 7.5 ms, and a flip angle of 90°. T1w opGRE sequences were acquired in a subgroup of 37 patients at Week 48 only.

*Definition of MRI lesions*. Fatty lesions and erosions were analyzed in the scope of this report. Fatty lesions were defined according to the ASAS definition[6]. Briefly, they are characterized by an increased signal on unenhanced T1w MR images in a paraarticular location within the bone marrow.

Erosions were scored on T1w TSE and opGRE images of the SIJ. According to ASAS definitions, erosions are of low signal intensity on T1w images and defined as bony defects at the joint margin[6]. As an extension of this ASAS definition, we determined that these bony defects had to be located at the subchondral plate of the joint, with a clearly visible cortical break on at least 2 adjacent slices. In our study, signal changes of surrounding bone marrow (e.g., fatty marrow changes or bony sclerosis) are not part of the definition of erosions. Further, as mentioned in the ASAS definition, confluence of erosions may be seen as pseudowidening of the SIJ[6].

*Fatty lesions*. Fatty lesions were evaluated on T1w TSE images under application of 2 different scoring systems designated as the simple (SBM) and comprehensive Berlin scoring methods (CBM). The SBM evaluates presence or absence of fatty lesions (0: no fatty lesions present; 1: fatty lesions present), while the CBM quantifies fatty lesions on a 0–3 scale (0: no fatty lesions, 1: ≤ 33%, 2: 33% to 66%, 3: > 66% of the subchondral bone area in the respective quadrant). The sum score was calculated by addition of the 8 quadrant scores, ranging either from 0–8 for SBM or from 0–24 for CBM[23,24].

*Erosions*. The detection of erosions on T1w TSE and opGRE sequences was compared under application of the CBM, quantifying the number of erosions on a 0–3 scale (0: no erosions, 1: ≤ 33%, 2: 33% to 66%, 3: > 66% of the bony joint surface in the respective quadrant). For both MRI sequences, the sum score was calculated by addition of all quadrants, resulting in a patient sum score ranging from 0–24.

*MRI scoring*. Scoring was performed with the help of the open-source DICOM viewer software OsiriX (Pixmeo). For this analysis, T1w TSE and opGRE sequences of the SIJ were extracted from the whole-body MRI examination and were recoded and archived separately to ensure that readers cannot correlate their findings to other sequences. Reading was performed by 2 radiologists with 5 years of experience in musculoskeletal imaging (MK and LB), following written instructions describing the different scoring systems. At first, a training session was performed, comprising consensus discussions of typical findings for erosions and fatty lesions, as well as typical confounders such as anatomical variants, sclerosis, and indirect signs of osteitis (signal loss in T1w sequences). As a next step, a training set of 15 MRI examinations (not part of the study population) was scored independently by both readers, and results were reviewed and discussed (by KGH). After this calibration process, scoring was performed under application of specific assessment sheets (provided as supplementary download). To prevent recall bias, T1w TSE and opGRE sequences were scored in 2 separate scoring sessions, each consisting of 2 parts. Readers were blinded to examination timepoints and treatment groups. Session 1, part A, comprised scoring of fatty lesions according to the SBM. Afterward, part B comprised scoring of erosions using T1w TSE sequences. After an interval of 8 weeks, session 2 was conducted with scoring of fatty lesions on T1w TSE sequences according to the CBM in part A, and scoring of opGRE sequences for erosions as part B.

For the scoring process, each SIJ was divided into 4 quadrants, separating the iliac from the sacral part and the upper (anterosuperior) from the lower (posteroinferior) part of the SIJ. Quadrants were divided by a fictional horizontal line along the bottom of the first sacral neural foramina and these lines were virtually copied to other slices. Accordingly, per patient, 8 quadrants had to be evaluated (Figure 1)[15,23,24]. All slices depicting the SIJ cleft were taken into account for scoring.

*Statistical analysis*. Baseline characteristics of the 2 treatment groups were compared under application of the chi-square test and Mann-Whitney U test. P values < 0.05 were considered statistically significant. All calculations were performed using the patient sum scores, thus ranging from 0–8 (SBM) or 0–24 (CBM). Interreader agreement for the comparison of the 2 scoring methods (SBM vs CBM for fatty lesions) and the 2 MRI pulse sequences (T1w TSE vs opGRE for erosions) was determined by calculating intraclass correlation coefficients (ICC) for status scores at all 3 timepoints as well as for change scores. The agreement of the SBM and CBM was assessed by calculating Spearman's correlation coefficients for fatty lesion scores. Correlation values were defined as follows: 0–0.2, poor; 0.3–0.4, fair; 0.5–0.6, moderate; 0.7–0.8, strong; > 0.8, excellent agreement[25,26]. Standardized response means (SRM) between baseline and Week 48 were calculated for fatty lesion scores to determine sensitivity to change of both scoring methods; higher SRM represent higher responsiveness. Additionally, Bland-Altman plots were generated to visualize systematic differences between both readers. All calculations were conducted by the statistical department of the German Rheumatism Research Centre (www.drfz.de/en).

## RESULTS

*Descriptive statistics*. All 75 enrolled patients had active axSpA, shown by clinical measures and positive MRI, and were randomly assigned to the etanercept (n = 40) or SSZ treatment groups (n = 35). There were no significant statis-

Personal non-commercial use only. The Journal of Rheumatology Copyright © 2014. All rights reserved.



Downloaded on April 16, 2024 from www.jrheum.org

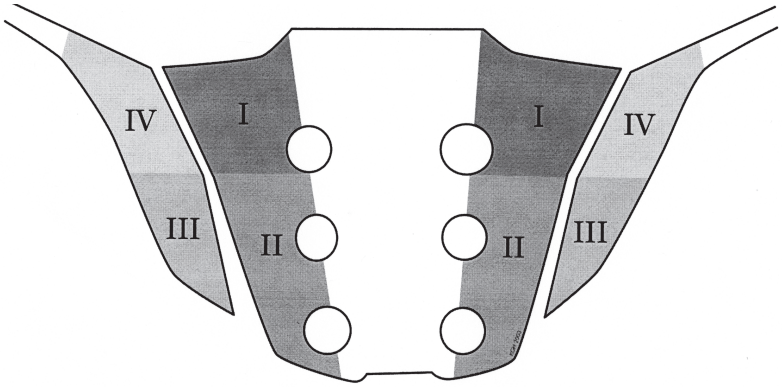


*Figure 1*. Magnetic resonance imaging scoring methodology for the evaluation of fatty lesions and erosions of the sacroiliac joints (SIJ): each SIJ is divided into 4 quadrants separated by the SIJ space and a fictional horizontal line positioned at the bottom of the first sacral neural foramina. Presence and amount of fatty lesions and erosions in each quadrant is assigned a score according to either the simple (SBM; 0: no lesions present; 1: lesions present) or comprehensive Berlin scoring methods (CBM; 0: no lesions present; 1: ≤ 33%, 2: 33-66%, 3: > 66% of the subchondral bone area), resulting in a sum score of either 0-8 or 0-24, respectively[23].

tical differences between both groups at baseline (Supplementary Table 1 available from the author on request).

*Fatty lesions*. For the evaluation of the SBM and CBM, fatty lesions were scored at baseline, Week 24, and Week 48. Applying the SBM, mean fatty lesion scores for both readers in the etanercept group were 4.59 and 5.19 at baseline and Week 48, respectively, while the CBM revealed mean fatty lesion scores of 6.59 and 7.64, respectively. In the SSZ group, mean fatty lesion scores dropped from 3.91 at baseline to 3.72 at Week 48 using SBM, and from 5.30 to 4.98 when applying the CBM (Table 1). Figure 2 gives an example of scoring results for fatty lesions.

The agreement between both scoring methods was very good to excellent (Spearman's correlation coefficients of 0.79–0.90; Supplementary Table 2 available from the author on request).

Sensitivity to change of both methods was estimated by calculating SRM. Under application of the CBM, SRM was 0.86 in patients treated with etanercept, although differences were evident between readers: SRM of 0.59 and 0.94 were calculated for reader 1 and reader 2, respectively. The application of the SBM resulted in an SRM of 0.59 for both readers and SRM of 0.49 and 0.44 for reader 1 and 2, respectively. In the SSZ group, application of both methods revealed a decrease of fatty lesion scores, resulting in negative SRM of –0.27 to –0.60 for CBM, while for SBM a sensitivity to change of –0.08 to –0.36 was found (Table 1).

Application of the SBM resulted in a good interreader agreement of status scores with ICC of 0.76–0.77, while the CBM showed ICC of 0.58–0.62 (Table 2). ICC for change scores were moderate for SBM (ICC of 0.42 and 0.48 for weeks 24 and 48, respectively), while under application of the CBM, ICC were 0.69 and 0.67, respectively (Table 3). Bland-Altman plots revealed smaller systematic differences between the readers under application of the CBM compared to the SBM (Supplementary Figure 1 available from the author on request).

*Erosions*. For the comparison of T1w TSE sequences with opGRE sequences, erosions were quantified under application of the CBM (Figure 3). Mean erosions scores were higher using the opGRE sequences compared to TSE sequences: the overall mean erosion score for T1w opGRE was 7.53 ± 4.55, while for TSE sequences a mean erosion score of 6.48 ± 3.70 was found. In detail, the mean erosion scores in the etanercept group were 8.22 ± 3.96 for opGRE and 7.10 ± 3.84 for TSE; the corresponding mean erosion scores in the SSZ group were 6.92 ± 5.01 and 5.77 ± 3.47, respectively. Interreader agreement for opGRE sequences was 0.65, while the ICC for T1w TSE sequences was 0.18 (Table 2). Bland-Altman plots showed fewer outliers and smaller systematic differences between scorers when using opGRE sequences (Supplementary Figure 1 available from the author on request).

## DISCUSSION

The data presented are part of a prospective, randomized multicenter trial (ESTHER), comparing the effects of etanercept versus SSZ over a period of 48 weeks in patients with axSpA[16,20]. While the diagnostic value of MRI in the detection of active inflammation in axSpA is undisputed, the detection and quantification of structural osseous changes (e.g., fat deposition, erosions, sclerosis, and ankylosis) in the course of disease represents a new focus of pharmaceutical and imaging studies. These structural osseous changes have been reported to appear in a certain order, beginning with active inflammation, which may lead to erosive bone destruction and possible alteration of the joint space width because of confluent erosions[6]. When inflammation decreases, fatty lesions eventually appear. During the later stages of axSpA, bony bridging may lead to partial or complete ankylosis of the affected regions[16,18,27]. Although

Personal non-commercial use only. The Journal of Rheumatology Copyright © 2014. All rights reserved.



Downloaded on April 16, 2024 from www.jrheum.org

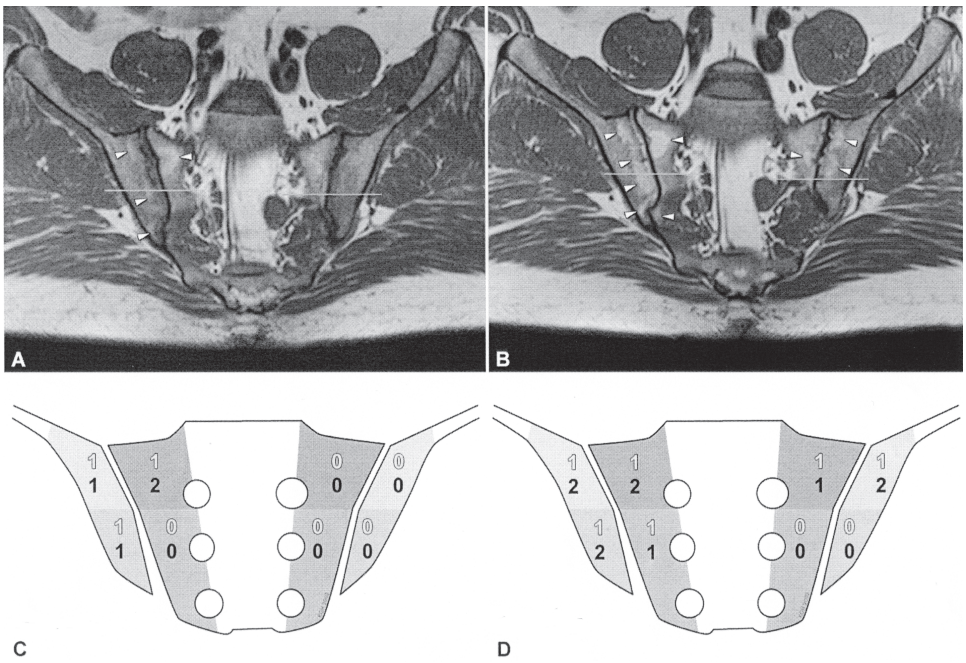


*Figure 2*. Magnetic resonance imaging (MRI) of the sacroiliac joints (SIJ) in coronal oblique orientation. Depiction of fatty lesions on T1-weighted turbo spin-echo sequences of the SIJ in the course of 1 year in a 36-year-old patient with axial spondyloarthritis. A. The baseline MRI shows a macular fatty lesion in quadrant I and slight fatty lesions in quadrants III and IV of the right SIJ (arrowheads). B. Followup MRI at Week 48 reveals progression of fatty lesions in all quadrants of the right SIJ and quadrants I and IV of the left SIJ (arrowheads). C. Baseline scoring of fatty lesions for each quadrant according to either the simple (SBM, white numerals) or the comprehensive Berlin scoring method (CBM, black numerals), resulting in a baseline sum score of 3 and 4 for SBM and CBM, respectively. D. Fatty lesion scores at Week 48 according to either SBM (white numerals) or CBM (black numerals). Note that the SBM fatty lesion sum score increases from 3 to 6, while under application of the CBM the fatty lesion sum score increases from 4 to 10, demonstrating that the differentiation of present lesions according to their extent, as performed under application of the CBM, results in a higher sensitivity to change compared to the SBM.

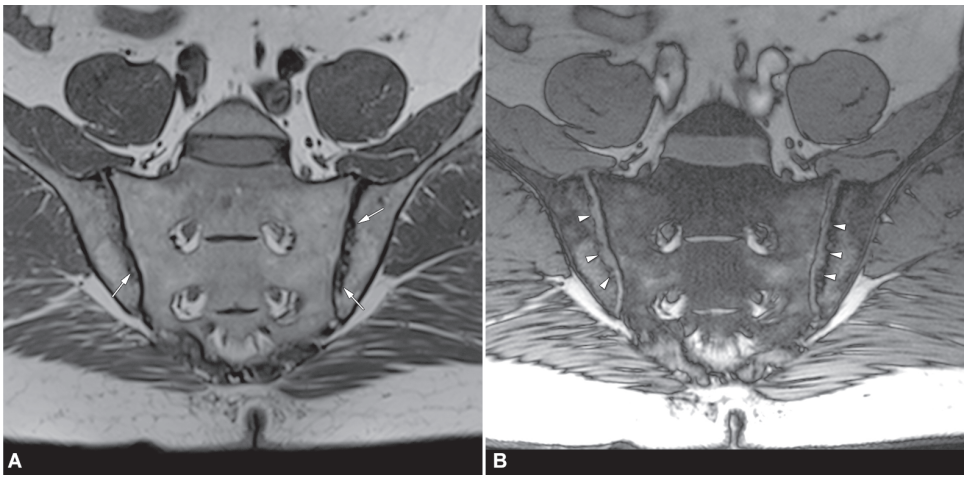


*Figure 3*. Magnetic resonance imaging of the sacroiliac joints (SIJ) in a 36-year-old patient with axial spondyloarthritis. A. Unenhanced T1-weighted turbo spin-echo (T1w TSE) sequence of the SIJ revealing joint areas with alterations of the iliac part of both SIJ suspicious for erosive osseous changes (arrows); however, bone margins are not clearly defined. B. Unenhanced T1w opposed-phase gradient-echo (T1w opGRE) sequence with clear definition of bone margins and a better delineation of erosions because of an improved contrast between joint space and bone (arrowheads); note that in areas of bone destruction on the basis of confluent erosions (in this case to be seen at the iliac part of both SIJ), T1w opGRE sequences, in contrast to T1w TSE sequences, can depict depth and fissuration of the respective joint area.

Personal non-commercial use only. The Journal of Rheumatology Copyright © 2014. All rights reserved.



Downloaded on April 16, 2024 from www.jrheum.org

*Table 1*. Sensitivity to change of the simple (SBM) versus comprehensive Berlin scoring method (CBM). Mean fatty lesion scores of both treatment groups at baseline and Week 48. Sensitivity to change of SBM and CBM is represented by standardized response means (SRM) calculated for each reader and both readers together. Scores are given as mean (SD).

| Fatty Lesion Scores | Etanercept Group | | | Sulfasalazine Group | | |
|---|---|---|---|---|---|---|
| | Baseline | Week 48 | SRM | Baseline | Week 48 | SRM |
| Reader 1 | | | | | | |
| SBM | 4.68 (2.99) | 5.23 (2.73) | 0.49 | 4.00 (2.62) | 4.00 (2.52) | –0.36 |
| CBM | 5.28 (4.77) | 6.34 (4.68) | 0.59 | 4.42 (4.82) | 4.30 (3.22) | –0.60 |
| Reader 2 | | | | | | |
| SBM | 4.50 (2.26) | 5.14 (2.34) | 0.44 | 3.82 (2.76) | 3.43 (2.51) | –0.08 |
| CBM | 7.90 (4.34) | 8.94 (4.52) | 0.94 | 6.18 (5.00) | 5.67 (4.45) | –0.27 |
| Reader 1 + 2 | | | | | | |
| SBM | 4.59 (2.47) | 5.19 (2.35) | 0.59 | 3.91 (2.54) | 3.72 (2.39) | –0.24 |
| CBM | 6.59 (4.12) | 7.64 (4.18) | 0.86 | 5.30 (4.54) | 4.98 (3.49) | –0.57 |

*Table 2*. Interreader agreement of both scoring methods, represented by intraclass correlation coefficients (simple vs comprehensive Berlin scoring methods for fatty lesions; T1w opGRE vs T1w TSE sequences for erosions). The T1w opGRE sequence was acquired in a subgroup of 37 patients at Week 48 only.

| Fatty Lesions | Baseline | Week 24 | Week 48 |
|---|---|---|---|
| SBM | 0.76 (95% CI 0.59–0.87) | 0.77 (95% CI 0.60–0.88) | 0.76 (95% CI 0.58–0.87) |
| CBM | 0.59 (95% CI 0.34–0.76) | 0.62 (95% CI 0.37–0.79) | 0.59 (95% CI 0.31–0.77) |
| Erosions | | | |
| T1 opGRE | N/A | N/A | 0.65 (95% CI 0.36–0.82) |
| T1 TSE | 0.34 (95% CI 0.03–0.59) | 0.37 (95% CI 0.05–0.63) | 0.18 (95% CI –0.16–0.49) |

SBM: simple Berlin scoring method; CBM: comprehensive Berlin scoring method; opGRE: T1-weighted opposed-phase gradient-echo sequences; TSE: T1-weighted turbo spin-echo sequences; N/A: not applicable.

the pathophysiology of axSpA is not well understood, the analysis of fatty lesions and erosions, which appear to be early structural osseous changes in the course of axSpA, has shown to be useful in the evaluation of the disease progress and efficacy of medical treatment[11,16].

As demonstrated by Song, *et al*, disappearance of inflammation and occurrence of fatty lesions within the course of the trial were significantly higher in the etanercept than in the SSZ treatment group[16]. However, in the reports by Song, *et al* and Althoff, *et al*, fatty lesions were evaluated as either present or absent per quadrant (according to SBM)[16,24]. This scale appeared inappropriate to show changes in the course of 1 year; therefore, the Berlin MRI scoring system was revised with a more comprehensive scale of 0–3 per quadrant (CBM).

We could show that both SBM and CBM can monitor the development of fatty bone marrow lesions, although the CBM is more sensitive to change. Mean fatty lesion scores during treatment with etanercept increased from 4.59 to 5.19 when applying the SBM (SRM of 0.59), and from 6.59 to 7.64 when applying the CBM (SRM of 0.86). However, a slight reduction of the interreader reliability has to be taken into account (ICC dropped from 0.76–0.77 to 0.58–0.62). Interestingly, in contrast to the etanercept group, fatty lesion scores decreased slightly in the SSZ group, which is most probably because of focal signal decrease due to newly occurring areas of inflammation. Depending on their number and extent, these lesions may reduce signal intensity to a degree that is represented by lower fatty lesion scores. Further, our analysis revealed moderate ICC for fatty lesion change scores under application of the SBM (ICC of 0.42 and 0.48 for weeks 24 and 48, respectively), while under application of the CBM, ICC were 0.69 and 0.67, respectively (Table 3), indicating that the more differentiated CBM is, especially if slight changes occur, the more easily it is applicable than the SBM. Corresponding Bland-Altman plots further demonstrate that the systematic difference between both readers is lower for CBM compared to the SBM (Supplementary Figure 1 available from the author on request).

To date, only a few studies have introduced a scoring method for structural osseous changes of the SIJ on MR images[14,15,28,29,30,31]. The Berlin research group initially introduced an MRI scoring system that basically referred to the New York criteria, i.e., structural osseous changes were globally scored in a 0–4 grading system without distinguishing between fatty lesions, erosions, sclerosis, or ankylosis[15,28,32]. The MISS (MR Imaging of Seronegative Spondylarthropathy) working group proposed a similar method, with evaluation of the iliac and sacral part of each SIJ[29,30]. The Leeds group introduced a grading system with evaluation of sclerosis and ankylosis on a 0–3 scale per

Personal non-commercial use only. The Journal of Rheumatology Copyright © 2014. All rights reserved.



Downloaded on April 16, 2024 from www.jrheum.org

*Table 3*. Change scores and corresponding intraclass correlation coefficients (ICC) for fatty lesions under comparison of the SBM and CBM. Data are mean ± SD (range) unless otherwise indicated.

| Change Scores — Fatty Lesions | Week 24–Baseline | Week 48–Baseline |
|---|---|---|
| SBM | | |
| Etanercept, n = 40 | | |
| Reader 1 | 0.42 ± 1.13 (2–4) | 0.34 ± 1.08 (2–4) |
| Reader 2 | 0.53 ± 1.08 (2–3) | 0.54 ± 1.15 (2–3) |
| Reader 1 + 2 | 0.47 ± 0.93 (2–3.5) | 0.44 ± 0.95 (1.5–3.5) |
| Sulfasalazine, n = 35 | | |
| Reader 1 | 0.15 ± 0.99 (1–3) | 0.11 ± 1.13 (2–4) |
| Reader 2 | 0.07 ± 1.14 (2–3) | 0.04 ± 1.00 (2–2) |
| Reader 1 + 2 | 0.11 ± 0.89 (1.5–2) | 0.07 ± 0.93 (1–3) |
| Interreader agreement | | |
| ICC (95% CI) | 0.42 (0.19–0.6) | 0.48 (0.27–0.65) |
| CBM | | |
| Etanercept, n = 40 | | |
| Reader 1 | 0.72 ± 2.15 (2–9) | 0.86 ± 2.05 (2–9) |
| Reader 2 | 0.69 ± 2.00 (2–8) | 0.89 ± 2.10 (3–7) |
| Reader 1 + 2 | 0.71 ± 1.94 (1.5–8.5) | 0.87 ± 1.91 (2.5–8) |
| Sulfasalazine, n = 35 | | |
| Reader 1 | 0.78 ± 1.80 (1–7) | 0.46 ± 1.75 (2–7) |
| Reader 2 | 0.22 ± 1.01 (2–2) | 0.32 ± 1.33 (2–4) |
| Reader 1 + 2 | 0.50 ± 1.31 (1–4.5) | 0.39 ± 1.38 (1–5.5) |
| Interreader agreement | | |
| ICC (95% CI) | 0.69 (0.54–0.80) | 0.67 (0.51–0.78) |

SBM: simple Berlin scoring method; CBM: comprehensive Berlin scoring method.

quadrant (0: absent, 1: ≤ 25%, 2: 25–75%, 3: > 75% of the articular surface)[33]. The Denmark group initially proposed an MRI grading system with separate evaluation of fat accumulation, erosions, joint space width, and sclerosis on a 0–3 scale and transformation into an overall score for joint destruction[14]. That study showed that the 0–3 grading method results in a good to excellent interreader agreement with regard to sclerosis, erosions, fat accumulation, and overall joint destruction[14]. More recently, this group proposed a similar grading system[34,35] that scores fatty bone marrow deposition per quadrant on a 0–3 scale [0: normal, 1: < 25%, 2: 25% to 50%, 3: > 50% of the joint area; additional score for lesion depth (0: < 1 cm, 1: > 1 cm)]; erosions are scored per half of each SIJ, and ankylosis is assigned a score of 0–2 per joint (0 = no ankylosis, 1 = partial, 2 = complete ankylosis). These scores can be transformed into a total chronic score of 0–48 per patient[34,35]. Weber, *et al* adapted the Spondyloarthritis Research Consortium of Canada (SPARCC) scoring system (originally developed for assessment of active inflammation in SIJ, with dichotomous grading of each quadrant on 6 adjacent MRI slices and additional scoring of lesion intensity and depth) for quantification of fat deposition and erosions, while ankylosis is assigned a score for each half of both SIJ[36]. Wick, *et al* modified the SPARCC method for the evaluation of joint space width, erosions, and subcortical cysts[11]. Sensitivity to change of the proposed scoring systems has not yet been assessed.

The second aim of our study was the comparison of unenhanced T1w TSE sequences, one of the standard sequences for MRI of the SIJ, with T1w opGRE sequences regarding the detection and quantification of erosions. We could show that the interreader agreement was much higher for opGRE images (ICC 0.65) than for TSE images (ICC 0.18–0.37), indicating that T1w opGRE sequences may be more useful for the evaluation of erosions in patients with axSpA than the usually applied T1w TSE sequences. Corresponding Bland-Altman plots demonstrate that under application of opGRE sequences, fewer outliers and smaller systematic differences occur between scorers compared to TSE sequences. However, compared to other studies that have assessed interreader agreement in the detection of erosions on T1w SE sequences, ICC in our study (0.18–0.37) appear unusually low, although even more experienced readers may also observe erosion ICC of about 0.40–0.60[10,12,37]. Additionally, low interreader agreement may occur because readers were blinded to other sequences of the same patient, such as STIR sequences, which was not the case in most of the other existing studies.

To date, only limited reports exist about the value of opGRE sequences in axSpA[6,8,15,38,39,40]. The authors mention the excellent contrast between the articular cartilage, subchondral plate, and adjacent bone marrow; however, the proposed imaging techniques have not been analyzed separately to demonstrate the superiority of 1 sequence compared to the other with regard to delineation of

Personal non-commercial use only. The Journal of Rheumatology Copyright © 2014. All rights reserved.



Downloaded on April 16, 2024 from www.jrheum.org

erosions. Further, GRE sequences are known to be susceptible to a variety of artifacts as shown in several veterinarian and human studies, leading to significantly greater subchondral bone thickness measures, underestimation of subchondral lesions, and false-negative scoring results[41,42,43,44]; although in our study, mean erosion scores and interreader agreement were higher for opGRE than for T1w TSE sequences. However, one of those veterinary studies found high sensitivity of GRE sequences regarding the detection of osteochondral defects, while their specificity was shown to be rather low[42].

Aside from T1w and T2*w GRE sequences, other noteworthy sequences in the detection of erosions include T2w sequences[8,13] and contrast-enhanced T1w fat-saturated SE sequences[13,15]. So-called cartilage sequences such as T2w GRE, unenhanced fat-saturated T1w sequences, 3-dimensional (3-D) FLASH, and 3-D double excitation in the steady-state (3D-DESS) sequences have been discussed to facilitate the detection of erosions[34,35,45,46]. Proton-density weighted sequences play an important role in the depiction of cartilage, menisci, ligaments, and tendons, especially in larger joints, and are predominantly used in orthopedic-traumatological MR protocols[43,47].

To our knowledge, our study is the first to assess the value of T1w opGRE in comparison to the usually applied T1w TSE sequences with regard to the detection and quantification of erosions in patients with rheumatic diseases. Unfortunately, T1w opGRE sequences were only acquired at 1 timepoint, so that their sensitivity to change was not assessable in our analysis. Comparison to healthy control subjects was not possible in the setting of this analysis of patients within the ESTHER trial[20] but should be performed prospectively in a future study.

The CBM appears to be a feasible MRI scoring method for the quantification of fatty lesions and erosions, with higher sensitivity to change compared to the SBM. Additionally, we could show that for the detection of erosions, T1w opGRE sequences appear to be more reliable than the usually applied T1w TSE sequences. More studies need to be conducted to further evaluate feasibility and sensitivity of the CBM for the assessment of structural osseous changes on MRI and to determine the value of T1w opGRE sequences regarding a more reliable detection of erosions in patients with axSpA.

## REFERENCES


1. Braun J, Bollow M, Sieper J. Radiologic diagnosis and pathology of the spondyloarthropathies. Rheum Dis Clin North Am 1998;24:697-735.
2. Dougados M, van der Linden S, Juhlin R, Huitfeldt B, Amor B, Calin A, et al. The European Spondylarthropathy Study Group preliminary criteria for the classification of spondylarthropathy. Arthritis Rheum 1991;34:1218-27.
3. van Tubergen A, Weber U. Diagnosis and classification in spondyloarthritis: identifying a chameleon. Nat Rev Rheumatol 2012;8:253-61.
4. Rudwaleit M, van der Heijde D, Landewe R, Listing J, Akkoc N, Brandt J, et al. The development of Assessment of SpondyloArthritis international Society classification criteria for axial spondyloarthritis (part II): validation and final selection. Ann Rheum Dis 2009;68:777-83.
5. Braun J, Baraliakos X. Imaging of axial spondyloarthritis including ankylosing spondylitis [Review]. Ann Rheum Dis 2011;70 Suppl 1:i97-103.
6. Rudwaleit M, Jurik AG, Hermann KG, Landewe R, van der Heijde D, Baraliakos X, et al. Defining active sacroiliitis on magnetic resonance imaging (MRI) for classification of axial spondyloarthritis: a consensual approach by the ASAS/OMERACT MRI group. Ann Rheum Dis 2009;68:1520-7.
7. Heuft-Dorenbosch L, Landewe R, Weijers R, Wanders A, Houben H, van der Linden S, et al. Combining information obtained from magnetic resonance imaging and conventional radiographs to detect sacroiliitis in patients with recent onset inflammatory back pain. Ann Rheum Dis 2006;65:804-8.
8. Yu W, Feng F, Dion E, Yang H, Jiang M, Genant HK. Comparison of radiography, computed tomography and magnetic resonance imaging in the detection of sacroiliitis accompanying ankylosing spondylitis. Skeletal Radiol 1998;27:311-20.
9. Braun J, Baraliakos X, Golder W, Hermann KG, Listing J, Brandt J, et al. Analysing chronic spinal changes in ankylosing spondylitis: a systematic comparison of conventional x rays with magnetic resonance imaging using established and new scoring systems. Ann Rheum Dis 2004;63:1046-55.
10. Weber U, Pedersen SJ, Ostergaard M, Rufibach K, Lambert RG, Maksymowych WP. Can erosions on MRI of the sacroiliac joints be reliably detected in patients with ankylosing spondylitis? — A cross-sectional study. Arthritis Res Ther 2012;14:R124.
11. Wick MC, Weiss RJ, Jaschke W, Klauser AS. Erosions are the most relevant magnetic resonance imaging features in quantification of sacroiliac joints in ankylosing spondylitis. J Rheumatol 2010;37:622-7.
12. Weber U, Lambert RG, Pedersen SJ, Hodler J, Ostergaard M, Maksymowych WP. Assessment of structural lesions in sacroiliac joints enhances diagnostic utility of magnetic resonance imaging in early spondylarthritis. Arthritis Care Res 2010;62:1763-71.
13. Bredella MA, Steinbach LS, Morgan S, Ward M, Davis JC. MRI of the sacroiliac joints in patients with moderate to severe ankylosing spondylitis [Clinical Trial]. AJR Am J Roentgenol 2006;187:1420-6.
14. Puhakka KB, Jurik AG, Egund N, Schiottz-Christensen B, Stengaard-Pedersen K, van Overeem Hansen G, et al. Imaging of sacroiliitis in early seronegative spondylarthropathy. Assessment of abnormalities by MR in comparison with radiography and CT. Acta Radiol 2003;44:218-29.
15. Hermann KG, Braun J, Fischer T, Reisshauer H, Bollow M. Die Magnetresonanz-Tomographie der Sakroiliitis: Anatomie, histologische Pathologie, MR-Morphologie und Sortier (German). Magnetic resonance tomography of sacroiliitis: anatomy, histological pathology, MR-morphology, and grading [review]. Der Radiologe 2004;44:217-28.
16. Song IH, Hermann KG, Haibel H, Althoff CE, Poddubnyy D, Listing J, et al. Relationship between active inflammatory lesions in the spine and sacroiliac joints and new development of chronic lesions on whole-body MRI in early axial spondyloarthritis: results of the ESTHER trial at week 48. Ann Rheum Dis 2011;70:1257-63.
17. Appel H, Sieper J. Spondyloarthritis at the crossroads of imaging, pathology, and structural damage in the era of biologics [Review]. Curr Rheumatol Rep 2008;10:356-63.
18. Chiowchanwisawakit P, Lambert RG, Conner-Spady B, Maksymowych WP. Focal fat lesions at vertebral corners on magnetic resonance imaging predict the development of new


Personal non-commercial use only. The Journal of Rheumatology Copyright © 2014. All rights reserved.



Downloaded on April 16, 2024 from www.jrheum.org

syndesmophytes in ankylosing spondylitis. Arthritis Rheum 2011;63:2215-25.
19. Poddubnyy D, Gaydukova I, Hermann KG, Song IH, Haibel H, Braun J, et al. Magnetic resonance imaging compared to conventional radiographs for detection of chronic structural changes in sacroiliac joints in axial spondyloarthritis. J Rheumatol 2013;40:1557-65.
20. Song IH, Hermann K, Haibel H, Althoff CE, Listing J, Burmester G, et al. Effects of etanercept versus sulfasalazine in early axial spondyloarthritis on active inflammatory lesions as detected by whole-body MRI (ESTHER): a 48-week randomised controlled trial. Ann Rheum Dis 2011;70:590-6.
21. Mager AK, Althoff CE, Sieper J, Hamm B, Hermann KG. Role of whole-body magnetic resonance imaging in diagnosing early spondyloarthritis [review]. Eur J Radiol 2009;71:182-8.
22. Althoff CE, Appel H, Rudwaleit M, Sieper J, Eshed I, Hamm B, et al. Whole-body MRI as a new screening tool for detecting axial and peripheral manifestations of spondyloarthritis. Ann Rheum Dis 2007;66:983-5.
23. Althoff CE, Feist E, Burova E, Eshed I, Bollow M, Hamm B, et al. Magnetic resonance imaging of active sacroiliitis: do we really need gadolinium? Eur J Radiol 2009;71:232-6.
24. Althoff CE, Sieper J, Song IH, Haibel H, Weiss A, Diekhoff T, et al. Active inflammation and structural change in early active axial spondyloarthritis as detected by whole-body MRI. Ann Rheum Dis 2013;72:967-73.
25. Landis JR, Koch GG. The measurement of observer agreement for categorical data. Biometrics 1977;33:159-74.
26. Shrout PE, Fleiss JL. Intraclass correlations: uses in assessing rater reliability. Psychol Bull 1979;86:420-8.
27. Lories RJ, Luyten FP, de Vlam K. Progress in spondylarthritis. Mechanisms of new bone formation in spondyloarthritis. Arthritis Research Ther 2009;11:221.
28. Bollow M, Braun J, Taupitz M, Haberle J, Reibhauer BH, Paris S, et al. CT-guided intraarticular corticosteroid injection into the sacroiliac joints in patients with spondyloarthropathy: indication and follow-up with contrast-enhanced MRI. J Comput Assist Tomogr 1996;20:512-21.
29. van der Heijde DM, Landewe RB, Hermann KG, Jurik AG, Maksymowych WP, Rudwaleit M, et al. Application of the OMERACT filter to scoring methods for magnetic resonance imaging of the sacroiliac joints and the spine. Recommendations for a research agenda at OMERACT 7. J Rheumatol 2005; 32:2042-7.
30. Marzo-Ortega H, Braun J, Maksymowych W, O'Connor P, Lambert R, Inman R, et al. Interreader agreement in the assessment of magnetic resonance imaging of the sacroiliac joints in spondyloarthropathy — the 1st MISS study [abstract]. Arthritis Rheum 2002;46 Suppl:S428.
31. Baraliakos X, van der Heijde D, Braun J, Landewe RB. OMERACT magnetic resonance imaging initiative on structural and inflammatory lesions in ankylosing spondylitis—report of a special interest group at OMERACT 10 on sacroiliac joint and spine lesions. J Rheumatol 2011;38:2051-4.
32. Braun J, Rudwaleit M, Hermann KG, Rau R. Imaging bei Morbus Bechterew (German – review). Imaging in ankylosing spondylitis. Z Rheumatol 2007;66:167-78.
33. Marzo-Ortega H, McGonagle D, O'Connor P, Hensor EM, Bennett AN, Green MJ, et al. Baseline and 1-year magnetic resonance imaging of the sacroiliac joint and lumbar spine in very early inflammatory back pain. Relationship between symptoms, HLA-B27 and disease extent and persistence. Ann Rheum Dis 2009;68:1721-7.
34. Madsen KB, Schiottz-Christensen B, Jurik AG. Prognostic significance of magnetic resonance imaging changes of the sacroiliac joints in spondyloarthritis—a followup study. J Rheumatol 2010;37:1718-27.
35. Madsen KB, Jurik AG. MRI grading method for active and chronic spinal changes in spondyloarthritis. Clin Radiol 2010;65:6-14.
36. Weber U, Lambert RG, Ostergaard M, Hodler J, Pedersen SJ, Maksymowych WP. The diagnostic utility of magnetic resonance imaging in spondylarthritis: an international multicenter evaluation of one hundred eighty-seven subjects. Arthritis Rheum 2010;62:3048-58.
37. Landewe RB, Hermann KG, van der Heijde DM, Baraliakos X, Jurik AG, Lambert RG, et al. Scoring sacroiliac joints by magnetic resonance imaging. A multiple-reader reliability experiment. J Rheumatol 2005;32:2050-5.
38. Bollow M, Braun J, Hamm B, Eggens U, Schilling A, Konig H, et al. Early sacroiliitis in patients with spondyloarthropathy: evaluation with dynamic gadolinium-enhanced MR imaging. Radiology 1995;194:529-36.
39. Bollow M, Braun J, Kannenberg J, Biedermann T, Schauer-Petrowskaja C, Paris S, et al. Normal morphology of sacroiliac joints in children: magnetic resonance studies related to age and sex. Skeletal Radiol 1997;26:697-704.
40. Bollow M, Hermann KG, Biedermann T, Sieper J, Schontube M, Braun J. Very early spondyloarthritis: where the inflammation in the sacroiliac joints starts [case reports]. Ann Rheum Dis 2005;64:1644-6.
41. Werpy NM, Ho CP, Pease AP, Kawcak CE. The effect of sequence selection and field strength on detection of osteochondral defects in the metacarpophalangeal joint. Vet Radiol Ultrasound 2011; 52:154-60.
42. Smith MA, Dyson SJ, Murray RC. Reliability of high- and low-field magnetic resonance imaging systems for detection of cartilage and bone lesions in the equine cadaver fetlock. Equine Vet J 2012;44:684-91.
43. Roemer FW, Frobell R, Hunter DJ, Crema MD, Fischer W, Bohndorf K, et al. MRI-detected subchondral bone marrow signal alterations of the knee joint: terminology, imaging appearance, relevance and radiological differential diagnosis [review]. Osteoarthritis Cartilage 2009;17:1115-31.
44. McGibbon CA, Bencardino J, Palmer WE. Subchondral bone and cartilage thickness from MRI: effects of chemical-shift artifact. MAGMA 2003;16:1-9.
45. Weber U, Ostergaard M, Lambert RG, Maksymowych WP. The impact of MRI on the clinical management of inflammatory arthritides. Skeletal Radiol 2011;40:1153-73.
46. Algin O, Gokalp G, Ocakoglu G. Evaluation of bone cortex and cartilage of spondyloarthropathic sacroiliac joint: efficiency of different fat-saturated MRI sequences (T1-weighted, 3D-FLASH, and 3D-DESS). Acad Radiol 2010;17:1292-8.
47. Schaefer FK, Kurz B, Schaefer PJ, Fuerst M, Hedderich J, Graessner J, et al. Accuracy and precision in the detection of articular cartilage lesions using magnetic resonance imaging at 1.5 Tesla in an in vitro study with orthopedic and histopathologic correlation. Acta Radiol 2007;48:1131-7.

Personal non-commercial use only. The Journal of Rheumatology Copyright © 2014. All rights reserved.



Downloaded on April 16, 2024 from www.jrheum.org